Mode Locking at THz Repetition Frequencies using Lasers with Phase Shifted Sampled Gratings

Lianping Hou*, Song Tang, Bin Hou, John H. Marsh
School of Engineering, University of Glasgow, Glasgow, G12 8QQ, U.K
**Corresponding author: lianping.hou@glasgow.ac.uk*

Abstract: Mode-locking at repetition frequencies of 800 GHz and 1 THz is reported in pi-phase-shifted sampled grating distributed-Bragg-reflector (DBR) lasers. The effective coupling coefficient of the phase-shifted gratings is twice that of conventional sampled grating DBRs.
OCIS codes: (140.4050) Mode-locked lasers; (140.5960) Semiconductor lasers; (320-7090) Ultrafast lasers; (050.5080) Phase shift.

Conventional sampled grating distributed-Bragg-gratings (C-SGDBRs) are commonly used in four-section DBR lasers with an extended tuning range [1]. More recently they have been used to determine precisely the wavelength spacing in arrays of distributed feedback (DFB) lasers for use in WDM systems [2], and as the reflectors in THz repetition frequency (F_r) semiconductor mode locked lasers (MLLs) [3]. However, the effective coupling coefficient, κ, of a C-SGDBR (Fig. 1(b)) is inevitably reduced substantially from that of a uniform grating because much of the sampled grating period has no grating. The use of π-phase shifted (PPS) gratings can overcome this limitation, as previously demonstrated in fiber lasers [4]. Recently we have reported mode-locking at 620 GHz, in 1.5 µm semiconductor lasers, comparing π-phase shifted SGDBR (PPS-SGDBR) and C-SGDBR MLLs. We confirmed the PPS gratings have an increased effective κ [5]. Here we demonstrate still higher F_r, – i.e., 800 GHz and 1 THz – taking MLL operation well into the ITU defined THz frequency band (275 GHz to 3 THz).

Figure 1(a) illustrates the device structure and dimensions of the each component. The design is based on ridge waveguides, with side-wall gratings in the DBR sections, fabricated using only a single electron beam lithography (EBL) step. The saturated absorption section is 20 µm long, the gain section is 960 µm long, and the PPS-SGDBR section is 648 µm long. The 600 µm long SOA was designed as a curved waveguide terminating at an angle of 10° relative to the normal direction of the facet with the ridge width tapering from 2.5 µm to 6 µm. The 0th order grating period (Λ) is 244 nm. Figure 1 (b) shows the structures of a C-SGDBR and a PPS-SGDBR. When the duty cycle of the PPS-SGDBR is chosen to be P_1/P=0.25(P is the sampling period, and P_1 is the length of the grating burst), the different order peaks in the reflection spectrum are most uniform. For the scenario of 800 GHz, P=54 µm, P_1=13.5 µm, and the number of the sampling periods N_s is 12. The effective κ of the PPS-SBG is expected to be twice ((54-2×13.5)/13.5=2) that of a C-SGDBR and half ((54-2×13.5)/54=0.5) that of a uniform grating. For the scenario of 1 THz, P=43.2 µm, P_1=11 µm, N_s = 15, the effective κ of the PPS-SBG is expected to be around twice ((43.2-

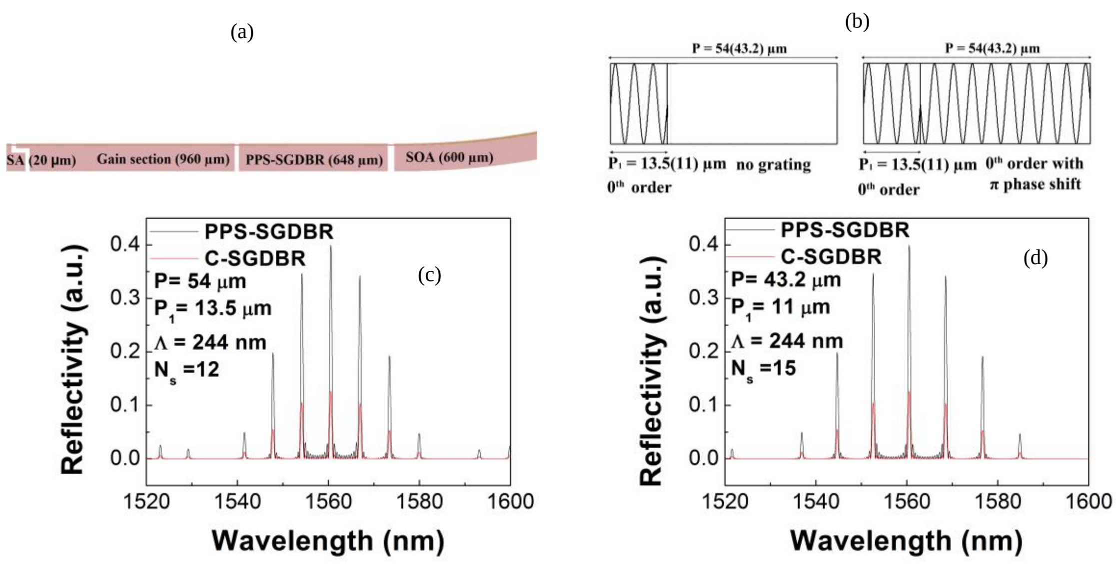

Fig.1 (a) Device structure based on PPS-SGDBR to produce 800 GHz and 1THz repetition frequency pulse trains, (b) grating structures of C-SGDBR and PPS-SGDBR, (c) simulated reflectivity of the 800 GHz and (d) 1THz PPS-SGDBR.

2×11)/11=1.93) that of a C-SGDBR and half (((43.2-2×11)/43.2=0.49) that of a uniform grating. Transfer matrix simulations of the reflectivity of the two scenarios of PPS-SGDBR and a comparison with the corresponding C-SGDBRs are shown Fig.1(c) and (d) respectively, and confirm the above analysis.

The epitaxial structure and fabrication processes are similar to those described in [3]. Figure 2 shows the measured lasing spectra and the corresponding autocorrelation trances for the case of 800 GHz and 1.0 THz MLLs, with the bias conditions indicated in the caption. In our devices, the uniform grating κ≈23.2 cm^{-1}, lower than the designed value of 80 cm^{-1} because of the reactive-ion etch lag effect. However, the effective κ of the PPS-SBG is nearly twice of that of the C-SGDBR, giving a clearer and sharper reflection comb with a wavelength spacing of 6.6 nm (Fig.2 (a)) and 8.1 nm (Fig.2(c)) for the 800 GHz and 1 THz cases respectively. The average period of the pulse train was measured to be 1.25 ps and 1.0 ps, corresponding to an F_r of 800 GHz (Fig.2 (b)) and 1 THz (Fig.2 (d)).

In conclusion, 800 GHz and 1 THz F_r MLLs based on PPS-SGDBRs have been successfully demonstrated. Device fabrication is straightforward using conventional EBL and the laterally coupled gratings require no regrowth. Because of the increased effective coupling coefficient of the PPS-SGDBR compared with the C-SGDBR, the length of the PPS-SGDBR and the total length of monolithically SGDBR MLLs could be reduced.

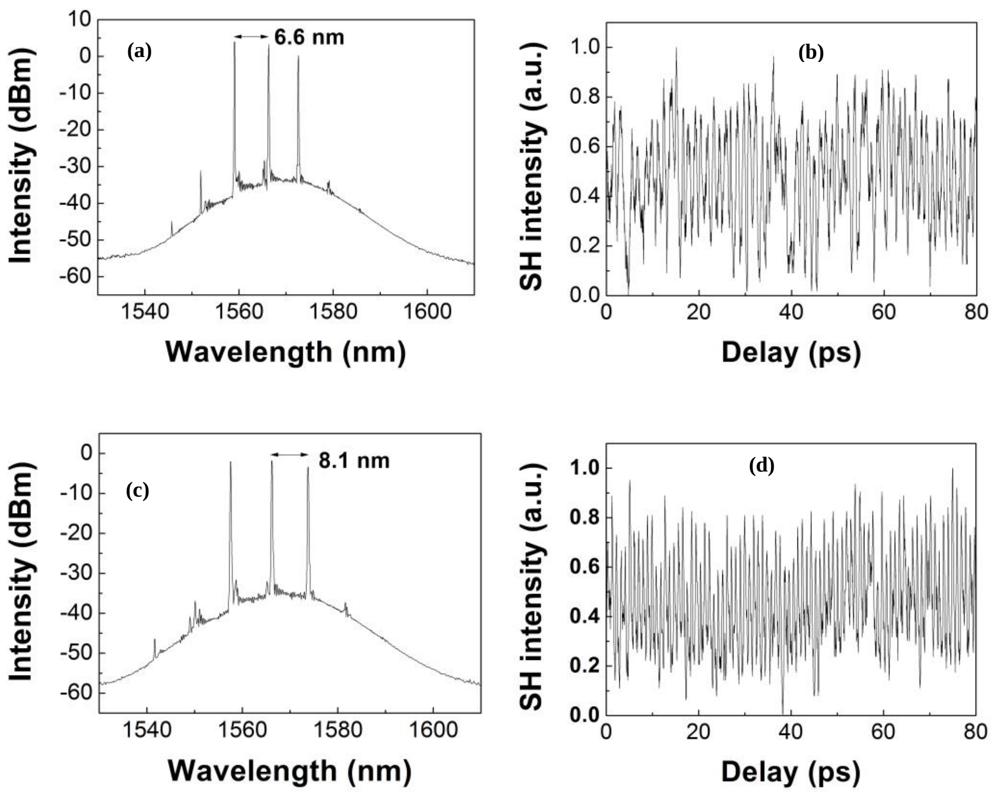

Fig.2 (a) measured optical spectrum and (b) autocorrelation trace of the 800 GHz MLLs under V_{SA} = -3V, I_{Gain} =180 mA, I_{DBR}=10 mA, I_{SOA} =100 mA; (c) measured optical spectrum and (d) autocorrelation traces of the 1 THz MLLs under V_{SA} = -3V, I_{Gain} =232 mA, I_{DBR}=10 mA, I_{SOA} =100 mA.

References

[1] V. Jayaraman, Z. M. Chuang, and L.A. Coldren, "Theory, design, and performance of extended tuning range semiconductor lasers with sampled gratings," IEEE J. Quantum Electron., **29**, 1824-1834 (1993).
[2] Y. Shi, S. Li, X. Chen, L. Li, J. Li, T. Zhang, J. Zheng, Y. Zhang, S. Tang, L. Hou, J. H. Marsh, B. Qiu, "High channel count and high precision channel spacing multi-wavelength laser array for future PICs," Scientific Reports, **4**, 7377 (2014).
[3] L. Hou, M. Haji, J. H. Marsh, "Mode locking at Terahertz frequencies using a distributed Bragg reflector laser with a sampled grating," Opt. Lett. **38**, 1113-1115 (2013).
[4] J. Li, Y. Cheng, Z. Yin, L. Jia, X. Chen, S. Liu, S. Li and Y. Lu, "A multiexposure technology for sampled Bragg gratings and its applications in dual-wavelength lasing generation and OCDMA en/decoding," IEEE Photon. Technol. Lett., **21**, 1639-1641 (2009).
[5] L. Hou, S. Tang, and J. H. Marsh, "THz repetition frequency mode-locked laser using novel sampled gratings," in Lasers and Electro-Optics Europe & European Quantum Electronics Conference (CLEO/Europe-EQEC, 2017 Conference on), 2017, pp. 1-1.